

Dosimetry calculations based on MCNP code of the Training Reactor of Budapest University of Technology and Economics

Tran Duy Tap¹, Nguyen Tien Cuong², Papp Ildikó³, Gábor Náfrádi³,

¹Faculty of Physics and Engineering Physics VNUHCM-University of Science

227 Nguyen Van Cu District 5, Ho Chi Minh City, Viet Nam, tel.: +84 121 8071 485

²Faculty of Physics, VNU-University of Science

334 Nguyen Trai, Thanh Xuan, Ha Noi, Viet Nam, tel.: +84 43-8584615

³Institute of Nuclear Techniques (NTI), Budapest University of Technology and Economics (BME)

H-1111 Budapest, Hungary, +36-1-463 1967

This study presents the work of Vietnamese experts performed during a twelve-week training at BME. The MCNP code was used to model the BME Training Reactor. Dose rates were determined for neutrons and photons for the top of the reactor, the outer of the concrete wall as well as the inside of the vertical water irradiation channels and the pneumatic rabbit system at different power levels and in case of the loss of water. Calculated data are in good agreement with the measured values.

Introduction

The governments of Vietnam and Hungary have accepted cooperation on the training project in the field of nuclear energy. According to the project, many advanced courses have been arranged to provide the comprehensive overview of the technical-scientific background for the construction and operation of a Nuclear Power Plant (NPP). Theoretical background, human resource needs, associated training programs and many other advanced courses were held on reactor physics and related fields. As one of the advanced courses of the project, the "Application of Monte Carlo methods in reactor physics" at Budapest University of Technology and Economics (BME) has been conducted to calculate the problems of criticality, biological protection, and dosimetry.

Related to the problems of reactor physics, the precise calculation of dose rates of neutrons and photons is highly desired to perform neutron activation analysis, production of radioisotopes, determination of safety in standard operation circumstance or even in accident situations, criticality calculation or evaluation of many other processes [1, 2]. Especially, during the planning and the operation of the reactor, it is a crucial task to make a safety analysis. One possible accident is the loss of cooling water surrounding the reactor core what may induce severe problems, including loss of the biological shielding which leads to the increase of dose rate surrounding the reactor. In most cases it is impossible to conduct preliminary experiential measurements of dose rate in accident situations. One of the possible solutions to this problem is to use simulation codes.

The Monte Carlo N-Particle (MCNP) transport code has an extensive history at Los Alamos National Laboratory dating

from the 1940s. The first released version for public distribution is MCNP3 in 1983 and then MCNP4B in 1996, MCNPX in 1997 and MCNP4C in 2001-2002 [3-5]. The latter versions include more and more particle types and extend many applications. MCNP5 was released as a result of enhancing by combination of MPI message passing and OpenMP threading to support large scale parallelism [6]. The latest current version, MCNP6, can be described as a fusion of MCNP5 and MCNPX capabilities, but it has much more new advanced features [7]. MCNP codes are general-purpose three dimensional simulation tools for the transport of 37 different particle types among which neutrons, photons and electrons are widely treated with a large-scale energy regime of 10^{-1} – 20 MeV, 10^6 – 10^2 GeV, and 10^6 – 1 GeV, respectively. The code allows calculating the criticality, shielding, dosimetry, designing, detector response, and many other applications. Especially, advanced features of MCNP code allow the calculation of k_{eff} eigenvalues for fissile systems using the KCODE option and particle flux distribution and thus dose rate even at severe operation conditions which are impossible to analyze by the experiments.

Although BME-Reactor has been safely operated over four decades, it is necessary to examine the dose rates surrounding the reactor under assumption of several severe operation conditions such as loss of cooling water. Thus, the present work aims to calculate the dose rates of neutron and photon at different positions inside the vertical water irradiation channels and the pneumatic rabbit system using the MCNP code with an assumption that the cooling water is dropped to different levels. Besides, the dose rates at the outer wall of the concrete layers and at the top of the reactor with different values of reactor power under the normal operation are also determined and evaluate the safety.

Materials and methods

The Training Reactor of the Budapest University of Technology and Economics (BME-Reactor) reached a critical state for the first time in 1971. It is specially designed for use in neutron activation analysis, production of short-lived radioisotopes, and for education and training [8, 9]. BME-Reactor has a pool-type water-moderated structural configuration, a nominal maximum thermal power rating of 100 kW, and the maximum thermal neutron flux of 2×10^{12} n/cm²/s. The cylinder-shaped tank is 1400 mm in diameter and filled with desalted water while the coolant level is 5750 mm. The current core of the reactor is fueled by UO₂ in magnesium matrix enriched to 10% in Al-alloy cladding whose thickness is 1.5 mm. It has a total number of 24 fuel assemblies which together contain 369 pieces of EK-10 type fuel. The EK-10 fuel pins are 10 mm in diameter with an active length of 500 mm and an inactive length of 50 mm at each end of the fuel rods.

Based on the real structure of the BME-Reactor, a simplified MCNP geometry model was constructed as shown in the Figure 1. The reactor core is surrounded by water in a sandwiched aluminum (2 cm)-air (3 cm)-iron (1 cm) tank. Shielding concretes are arranged at the outer of the reactor core for radiation protection.

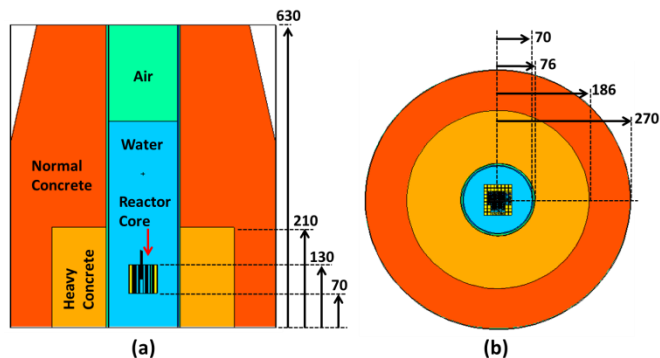


Figure 1. MCNP geometric model of the BME-Reactor: (a) side view, (b) cross-section top view. The dimension of various sizes showed in the figure is in centimeters

The BME-Reactor has one manual, one automatic, and two safety control rods, one fast pneumatic rabbit system, one thermal rabbit system, and irradiation channels in water and graphite as shown in Figure 2. The inner part of the manual control rod is made from boron carbide (1.8 cm of diameter) while the outer part is iron (0.1 cm of thickness). The automatic one includes an iron tube (1.8 cm of inner diameter, 2.0 cm of outer diameter) covered by cadmium (0.001cm of thickness) and the inner part of the iron tube is air. The full length of these control rods is 64 cm and the length of cover materials is 60 cm. The detailed components and information about materials are shown in Table 1.

MCNP code is a very powerful and versatile tool for nuclear reactor simulation. It can be used for calculations of multiplication factor, reaction rate distribution, power peaking factors, shielding, neutron fluxes, dose rate, spectra, and many other problems. Its main advantage is the ability to handle complicated geometries. Thus, the code is used to investigate the dosimetry of a whole nuclear reactor in operation. However, it should be noted that MCNP is a general purpose code.

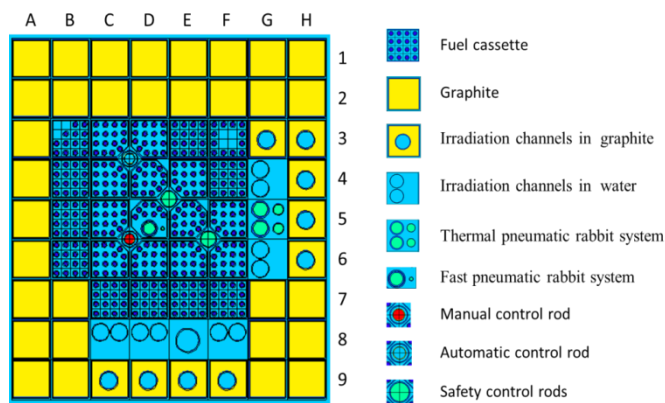


Figure 2. Cross-section top view of MCNP model of BME-Reactor core

It is therefore not optimized for any situations. In cases of dose rate calculation of neutron and photon at the top and outer of a nuclear reactor, the obtained results had low precision (high variance). This is due to the fact that Monte-Carlo simulation is a stochastic process and that always induces a statistical error in obtained results. The numbers of escaped particles from core to outer shielding concrete are not large enough to satisfy statistical tests. In this case, long computational time is needed to achieve statistically reliable results. There are many possible variance reduction techniques to solve above problem such as implicit capture, geometry splitting and Russian roulette, weight windows, weight cut-off, etc. Among them, geometry splitting and Russian roulette with suitable particle importance are simple but effective techniques. With these techniques, values of so called "importance" are assigned to each cell. All particles have a statistical weight of 1 when starting as a source particle. When a particle moves from a cell with a certain importance to a cell with a higher importance, the particle is split into multiple particles according the ratio of the cell importance to provide better sampling and the weight of the original particle is divided equally among the new particles. If particles move to a cell with lower importance, they are killed in unbiased way by Russian roulette. Splitting may increase the calculation time but decrease variance [10].

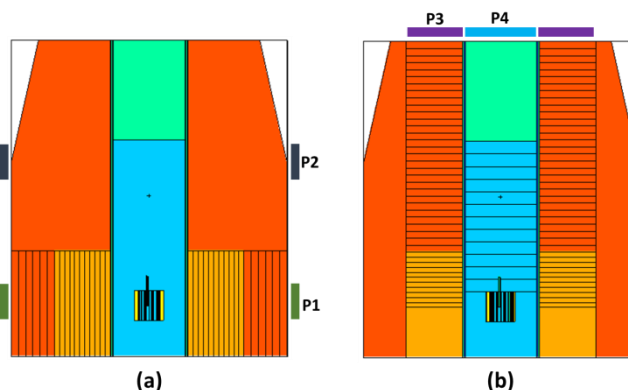


Figure 3. Schematic of split model for calculating dose rates: (a) outer concrete and (b) at the top of reactor

In order to calculate the dose rates at the outer shielding concrete wall of the BME-Reactor, heavy concrete and normal concrete regions are split into sub-layers with a thickness of 10 cm and 14 cm, respectively as shown in the Figure 3a. The P₁ and P₂ ring-shape cells, with 70 cm of height, 270 cm of

inner radius, and 271 cm of outer radius are constructed for dose rate calculations. Similarly, a part of heavy concrete, normal concrete, and the water layer at the upper reactor core are also split vertically into sub-layers of 10 cm, 14 cm, and 25cm, respectively for calculating the dose rates at the top of the reactor (Figure 3b). The P₃ cell is a thin ring-shape with 1 cm of height, 70 cm of inner radius, and 186 cm of outer radius. The P₄ cell is a thin disk with 1 cm of height and 70 cm of radius. In the calculations, particle importance of each sub-layer was determined to keep particle populations of the sub-layer nearly constant.

Table 1: Material detail used in the MCNP models

| | | |
|---|-----------------------------|-----------------------------|
| Fuel: $\rho = 5.45719438 \text{ g/cm}^3$ | | |
| ²³⁵ U -0.076126 | ²³⁸ U -0.6892785 | ²³⁴ U -6.052e-4 |
| C -3.5208e-3 | ¹⁶ O -0.1064826 | Mg -0.1239809 |
| ¹⁰ B -1.194e-6 | ¹⁰ B -1.194e-6 | |
| Aluminum: $\rho = 2.698900 \text{ g/cm}^3$ Al 1.0 | | |
| Water: $\rho = 0.998207 \text{ g/cm}^3$ | | |
| ¹ H +0.06672 | ¹⁶ O +0.00336 | (mt3 LWTR.01) |
| Air: $\rho = 2.698900 \text{ g/cm}^3$ | | |
| C -0.000124 | ¹⁴ N -0.755268 | ¹⁶ O -0.231781 |
| Ar -0.012827 | | |
| Stainless Steel: $\rho = 7.860000 \text{ g/cm}^3$ | | |
| C -0.001400 | Si -0.009300 | ³¹ P -0.000420 |
| S -0.000280 | Cr -0.180000 | ⁵⁵ Mn -0.018600 |
| Fe -0.700000 | Co -0.090000 | |
| Cadmium: $\rho = 8.650000 \text{ g/cm}^3$ Cd 1.0 | | |
| Iron: $\rho = 7.874000 \text{ g/cm}^3$ Fe 1.0 | | |
| Graphite: $\rho = 1.70000 \text{ g/cm}^3$ C 1.0 (mt8 GRPH.01) | | |
| Heavy concrete: $\rho = 3.35000 \text{ g/cm}^3$ | | |
| ¹ H -0.003585 | ¹⁶ O -0.311623 | Mg -0.001195 |
| ²⁷ Al -0.004183 | Si -0.010457 | S -0.107858 |
| Ca -0.050194 | Fe -0.047505 | ¹³⁸ Ba -0.463400 |
| Normal concrete: $\rho = 3.35000 \text{ g/cm}^3$ | | |
| ¹ H -0.004530 | ¹⁶ O -0.512600 | ²³ Na -0.001195 |
| ²⁷ Al -0.035550 | Si -0.360360 | Ca -0.057910 |
| Fe -0.013780 | | |
| Boron Carbide: $\rho = 2.52000 \text{ g/cm}^3$ | | |
| ¹⁰ B +0.782610 | C +0.217390 | |

The flux and the dose rate have been calculated using a cell flux tally (F4 tally) along with DE, DF cards of MCNP. The dose function DF and dose energy DE cards are used for energy to dose conversion using ANSI/ANS-6.1.1-1977 data. Since MCNP results are normalized to one source particle, the result has to be properly scaled to compare with the measured quantities such as flux and dose rate. The following formula has been used to scale the calculated results (F4 flux tally, Φ_{F4}) [11]

$$\Phi \left[\frac{\text{neutron}}{\text{cm}^2 \cdot \text{s}} \right] = \frac{P[W] \bar{\nu} \left[\frac{\text{neutron}}{\text{fission}} \right]}{\left(1.6022 \times 10^{-13} \frac{\text{J}}{\text{MeV}} \right) w_f \left[\frac{\text{MeV}}{\text{fission}} \right]} \cdot \frac{1}{k_{\text{eff}}} \cdot \Phi_{F4} \left[\frac{1}{\text{cm}^2} \right]$$

where P is the reactor power, $\bar{\nu}$ is the average number of neutron per fission and w_f is an average released energy per fission. The element and/or isotopic compositions of all materials used in the MCNP calculations are presented in the Table 1.

Results and discussions

Flux calculations

Table 2 shows the values of the total neutron flux inside the vertical water irradiation channels (G4 and G6) and the pneumatic rabbit systems (C8, F8, E8, and D5) along with the k_{eff} at different water levels at the power of 100 kW. The values of k_{eff} approach the critical state at the positions of control rods immersing inside the reactor core of 18 cm. The order magnitude of total neutron flux in all the channels is ten to the twelfth 1/cm²s and that is good agreement with measured results [12]. When the water levels drop to 3 m from the original position, the total neutron flux did not change and thus inducing no effect on the values of k_{eff} . However, when the dropping water levels increase to 4 or 5 m, the very small changes of neutron flux were observed. As the results, the value of k_{eff} (0.99811 ± 0.00017) at the dropping water level of 5 m is quite lower than that of the critical state. These results indicate that the presented MCNP model describes well the geometries and the normal operation of the BME-Reactor.

Table 2: The total flux of neutron ($\times 10^{12} \text{ n/cm}^2 \times \text{s}$) at different positions inside the vertical water irradiation channels and the pneumatic rabbit systems as a function of the dropping water levels at the power of 100 kW

| Pos. | 5 (m) | 4 (m) | 3 (m) | 2 (m) | 1 (m) | 0 (m) |
|------------------|-----------------------------|-----------------------------|-----------------------------|-----------------------------|-----------------------------|-----------------------------|
| G4 | 3.22 | 3.11 | 3.14 | 3.14 | 3.14 | 3.14 |
| G6 | 2.79 | 2.74 | 2.71 | 2.71 | 2.71 | 2.71 |
| C8 | 2.83 | 2.87 | 2.86 | 2.86 | 2.86 | 2.86 |
| F8 | 1.89 | 1.89 | 1.86 | 1.86 | 1.86 | 1.86 |
| E8 | 2.38 | 2.31 | 2.33 | 2.33 | 2.33 | 2.33 |
| D5 | 6.97 | 6.93 | 6.86 | 6.86 | 6.86 | 6.86 |
| k_{eff} | 0.99811 \pm 0.00017 | 1.00259 \pm 0.00016 | 1.00259 \pm 0.00017 | 1.00259 \pm 0.00017 | 1.00259 \pm 0.00017 | 1.00259 \pm 0.00017 |

Calculations in concrete structures

The reactor is surrounded by concrete regions. In case of the Training Reactor one can find heavy and normal concrete.

Table 3 shows the important functions, particle populations, and corresponding relative errors in these split sub-layers of concretes in the normal operation (with full water level). When a parallel beam of particles goes through the material, the intensity decrease can be very roughly approximated by an exponential function. Thus, particle importance is chosen as the exponential functions of the concrete sub-layers index, $= I_0 e^{\mu i}$, where μ is the coefficient of increment. One can predict that the particle populations change slightly through both heavy and normal concrete sub-layers. These sub-layers have therefore enough particles to satisfy MCNP statistical tests, which result in their low corresponding relative errors. As mentioned in the section of Materials and methods, the

regions as shown in Figure 1. Heavy concrete and normal concrete areas are split into sub-layers (Figure 3a) and particle importance functions are assigned to these sub-layers in order to calculate dose rate at the outer of concrete walls. Geometry splitting with suitable particle importance functions is an effective technique for reducing variance. The calculated results of dose rates at P1 and P2 positions (Figure 3) clearly demonstrate this effect. The relative errors of dose rate calculations for photons and neutrons are 2.51% and 4.72%, respectively (at P1), and 60.53% and 99.99%, respectively (at P2) in the case the water level drops 5 m. If the geometry splitting and importance techniques are not applied, these error values are almost 100%, the obtained results thus are not reliable. The details of dose rates at P1 and P2 are shown in the Figure 4, the dose rates through split concrete sub-layers are shown in the Figure 5, and those will be discussed below.

Table 3: Importance functions (Imp.), particle populations (Pop.), and relative errors (Err.) in the split sub-layers of concretes of the MCNP dose rate calculations for photons and neutrons in the normal operation

| Index | | Heavy concrete | | | | | | | | | | Normal concrete | | | | | | |
|---------|-------------------------|--|------|------|------|------|------|------|------|------|------|---|------|------|------|------|------|------|
| | | 1 | 2 | 3 | 4 | 5 | 6 | 7 | 8 | 9 | 10 | 11 | 1 | 2 | 3 | 4 | 5 | 6 |
| Photon | Imp. | $I = 3e^{1.0i} (i = \overline{0,1, \dots, 10})$ | | | | | | | | | | $I = 133258e^{1.0i} (i = \overline{0,1, \dots, 5})$ | | | | | | |
| | Pop. (10 ⁶) | 6.05 | 3.29 | 2.62 | 2.07 | 1.65 | 1.36 | 1.15 | 0.99 | 0.86 | 0.76 | 0.70 | 0.23 | 0.23 | 0.19 | 0.16 | 0.31 | 0.25 |
| | Err. (%) | 0.14 | 0.20 | 0.27 | 0.34 | 0.43 | 0.53 | 0.66 | 0.82 | 1.04 | 1.29 | 1.60 | 1.90 | 2.19 | 2.46 | 2.73 | 2.89 | 2.92 |
| Neutron | Imp. | $I = 2e^{0.69i} (i = \overline{0,1, \dots, 10})$ | | | | | | | | | | $I = 5139e^{0.92i} (i = \overline{0,1, \dots, 5})$ | | | | | | |
| | Pop. (10 ⁴) | 3.16 | 3.37 | 4.13 | 4.44 | 4.55 | 4.48 | 4.21 | 3.79 | 3.38 | 2.98 | 2.75 | 2.29 | 2.34 | 2.33 | 2.23 | 2.05 | 1.51 |
| | Err. (%) | 1.79 | 2.08 | 2.38 | 2.67 | 2.99 | 3.37 | 3.74 | 4.04 | 4.43 | 4.82 | 5.26 | 5.69 | 6.05 | 6.63 | 7.34 | 7.91 | 8.57 |

Figure 4 shows the dose rates of neutrons and photons at the outer of the concrete wall (P1 according to Figure 3a) as a function of power under the normal operation of the reactor. The values of dose rate of both neutrons and photons are the same order at each power and exponentially increase with the power. The dose rate at Position 1 is quite low (~ 1 μSv/h) at the power of 30 kW and then reaches around 4 μSv/h at power of 100 kW. When the power drops down to 1 kW or even 10 kW, the dose rates were detected to be 0.04 μSv/h and 0.4 μSv/h, respectively. Such values of dose rates allow working several days or more at the position of P1. The dose rates at position P2 (according to Figure 3a) which is 210 cm higher than position P1 was also calculated. As expected, the dose rates are much lower there at any possible power levels of the reactor. The results indicate that one can work at the position P1 for several days or more at the power of 10 kW or lower while there is no limitation of working time at the position P2.

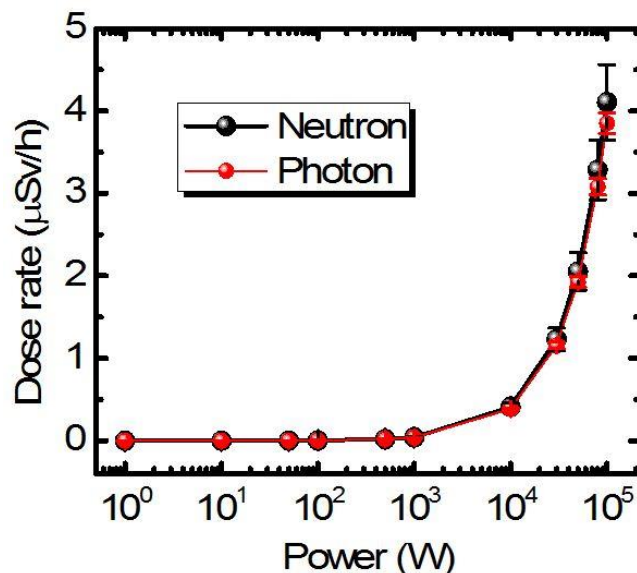


Figure 4. Dose rates of neutrons and photons at outer surface of the concrete wall (P1 according to Figure 3a) as a function of reactor power in normal operation of reactor

Dose rates of neutrons and photons as a function of distance from the inner protection concrete wall at the different dropping water levels and at the power of 100 kW were also determined as shown in Figure 5. The shielding concrete wall contains separately two layers: heavy concrete and normal concrete whose compositions are quite different as presented in Table 1. The obtained results in Figure 5a indicate that the transport of neutron does not change significantly when the particles go through the heavy and normal concrete.

On the other hand, two different slopes of the intensities of transported photons particles through two layers were clearly observed (Figure 5b). This is due to the sensitive effect of photon to different heavy elements contained in the heavy and normal concrete walls. The results in Figure 5 also indicate that the dose rates of both neutrons and photons at each sub-layer of heavy and normal concrete were not

affected when the water levels dropped by 4 m. However, when the water level dropped by 5 m, i.e., it was the same height as the reactor core, the dose rates dramatically increased by to one or two orders. Even at the position P2, the dose rates of neutrons and photons were calculated to be 201 and 354 $\mu\text{Sv/h}$ when the water level drops to 5 m. The results indicate that dropping the water level by 5 m (identical height to the center of reactor core) induces severe problem of significant increase of dose rate.

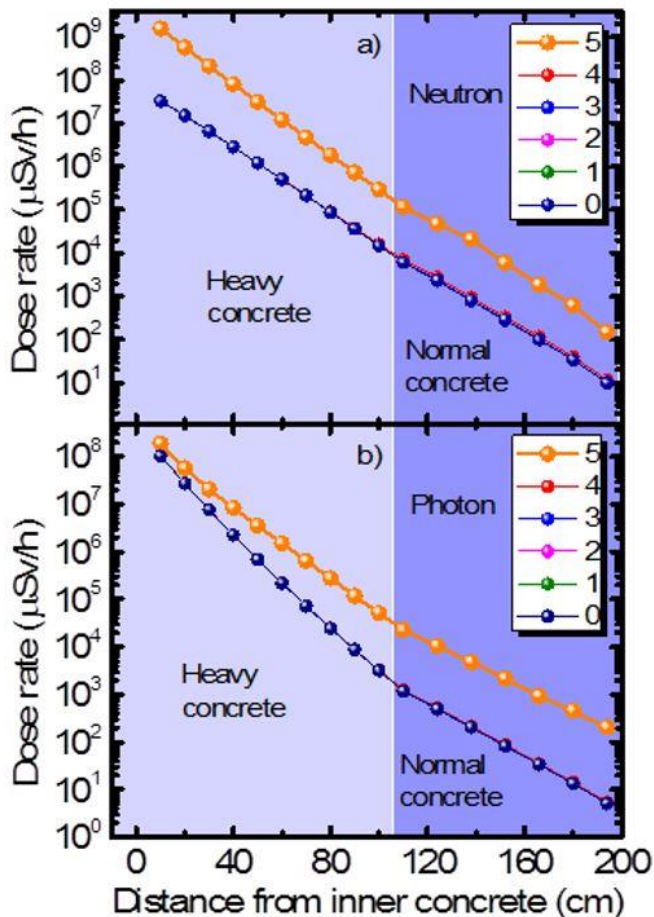


Figure 5. Dose rate of a) neutron and b) photon as a function of distance from the inner concrete wall at different dropping water levels (from 0 to 5 m as showed in the figure) and at the power of 100 kW

In order to calculate the dose rates at the top of the reactor, a part of heavy concrete, normal concrete, and the water layer at the upper reactor core were also split vertically into sub-layers (Figure 3b). The importance functions were also chosen as the exponential functions of these split sub-layers index to keep their particle populations nearly constant. The particle populations and corresponding relative errors in these sub-layers have been analyzed similarly in Table 3. For dose rate calculations at P4 position, exponential functions with coefficient of 1.6 for neutron and of 0.8 for photon were chosen for the water sub-layers. The calculated neutron dose rates of the water sub-layers show that the corresponding relative errors become too large from the 5th water sub-layers. This is due to the fact that water absorbs and reflects neutron very well. The result indicates that the neutron dose rates at P4 position are only reliable when water level is dropped by more than 4 m in our calculations. However, photon dose rate results at all sub-layers are reliable due to their

acceptable relative errors. For dose rate calculations at P3 position, exponential functions of heavy and normal concretes with different coefficients for neutron and photon were carefully chosen. However, the calculated dose rates at the P3 position have large relative error and will not be showed here. Thus, one of our tasks in the future is to apply several different methods to improve the variance to examine more properly the dose rate at position P3.

Figure 6 shows the values of measured and calculated dose rates normalized to the maximum dose rate as a function of reactor power at position P4 (according to Figure 3b) under the normal operation. When the power increases the normalized dose rates of measurement and calculation exponentially increase and have the quite similar behavior of changing.

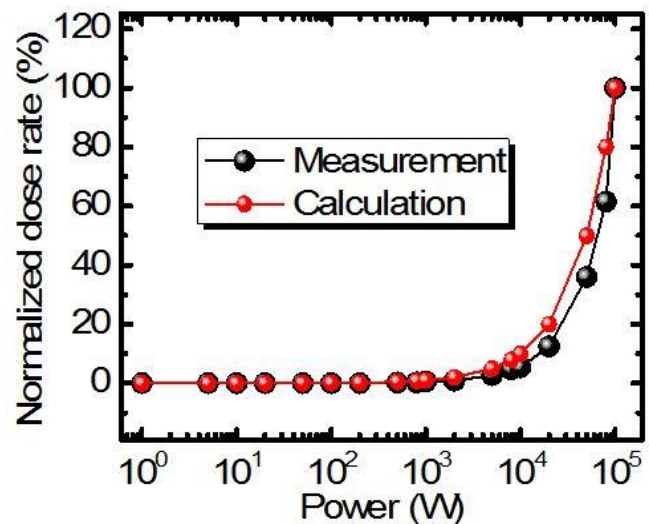


Figure 6. The normalized dose rate of photon of measurement and calculation at the top of reactor (Position P4 according to Figure 3b) as a function of reactor power in normal operation

Figure 7 shows the dose rate of neutrons and photons at the top of reactor (Position P4 according to Figure 3b) as a function of the dropping water level at the power of 100 kW. When the water level dropped from 4 to 5 m (measured from the top of the reactor), the huge dose rate values of neutron (1.1×10^4 – 5.3×10^8 $\mu\text{Sv/h}$) were detected at the position P4. However, when the water level dropped less than 3 m, the number of neutrons was detected to decrease significantly. On the other hand, the slope of the dose rate of photon as the function of the water level (3×10^6 – 5×10^7 $\mu\text{Sv/h}$) is much smaller in this region. In the entire interval the increase of the dose rate of photons can be described well by an exponential function with a coefficient of 3.49 ($R^2 = 0.952$). From the result of fitting, the dose rate of photons at any dropping water level can be calculated. This result is quite important to perform the shielding calculations or construct the safety system from the photon radiation at the top of reactor (position P4) when the accident of loss of cooling water occurs. In addition, above results also indicate that the photon particles predominantly contribute to the dose rate at the position P4.

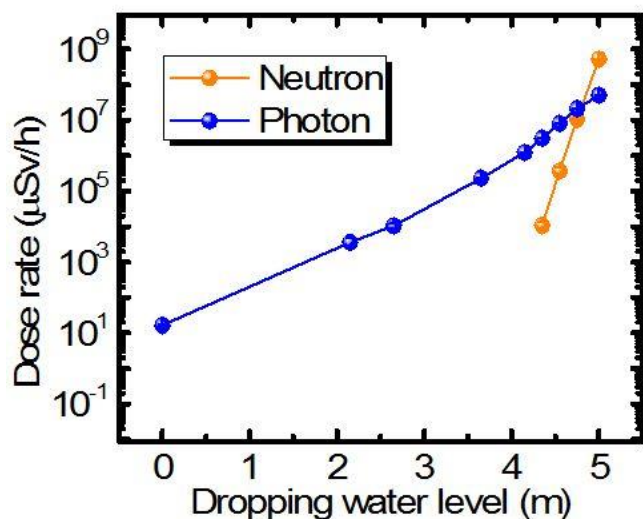


Figure 7. Dose rate of neutron and photon at the top of reactor (Positron P4) as a function of dropping water level at the power of 100 kW

Conclusions

Dose rates of neutrons and photons at the top of the reactor, on the outer surface of the concrete wall and inside region the vertical water irradiation channels and the pneumatic rabbit system at different powers were calculated in normal operation and during an accident using the MCNP code. The order magnitude of total neutron flux in all the irradiation channels is 10^{12} n/cm²s and that is in good agreement with measured results. In addition, the dose rate in all irradiation channels was not affected by the missing water level until the water level was dropped by 4 m. At the outer surface of the concrete wall (Position P1), the dose rates of 0.4 and 1 µSv/h at a power of 10 and 30 kW was obtained for neutrons and photons respectively. At the power of 100 kW, the dropping water level at 5 m (identical height to the center of reactor core) induces severe problem of significant increase in the dose rate. The result allows performing the shielding planning or constructing the safety system from the photon radiation at the top and the outer concrete wall of reactor when the accident of loss of cooling water occurs.

Acknowledgments

This work is the result of the training collaboration program between Vietnam and Hungary in the field of nuclear energy. Authors would like to thank the Ministry of Education and Training (MOET) of Vietnam and the Institute of Nuclear Techniques (NTI) of Budapest University of Technology and Economic (BME), Hungary for offering and sponsoring this training course.

References

- [1] Radiation protection aspects of design for nuclear power plants, Safety guide, No. NS-G-1.13, IAEA, 2005.
- [2] Radiation protection and radioactive waste management in the design and operation of research reactors, Safety guide, No. NS-G-4.6, IAEA, 2008.
- [3] Stefan Cerba, Jose Ignacio Marquez Damian, Jakub Lüley, Branislav Vrbán, Gabriel Farkas, Vladimír Necas, Jan Haščík, Comparison of thermal scattering processing options for S(α,β) cards in MCNP, *Annals of Nuclear Energy* 55 (2013) 18–22.
- [4] Joe W. Durkee Jr., MCNP geometry transformation and plotter equations, *Progress in Nuclear Energy* 61 (2012) 26–40.
- [5] T. Goorley, M. James, T. Booth, F. Brown, J. Bull, L. J. Cox, J. Durkee, J. Elson, M. Fensin, R. A. Forster, J. Hendricks, H. G. Hughes, R. Johns, B. Kiedrowski, R. Martz, S. Mashnik, G. McKinney, D. Pelowitz, R. Prael, J. Sweezy, L. Waters, T. Wilcox, T. Zukaitis, Features of MCNP6, *Annals of Nuclear Energy* 87 (2016) 772–783.
- [6] Joe W. Durkee Jr., Russell C. Johns, Laurie S. Waters, MCNP6 moving objects part I: Theory, *Progress in Nuclear Energy* 87 (2016) 104–121.
- [7] M. L. Fensin, J.D. Galloway, M. R. James, Performance upgrades to the MCNP6 burn up capability for large scale depletion calculations, *Progress in Nuclear Energy* 83 (2015) 186–190.
- [8] M. Balla, J. Gunneweg, Archaeological research at the institute of nuclear techniques, Budapest University of Technology and Economics: scholarly achievements of a prosperous long-term collaboration, *Archaeometry* 49, (2007) 373–381.
- [9] Khaled Sayed Mahmoud, Numerical modeling of reactivity excursion accidents in small light water reactors, PhD Thesis, Department of Nuclear Techniques, Institute of Nuclear Techniques Budapest University of Technology and Economics, 2006.
- [10] Marisa van der Walt De Kock, Variance reduction techniques for MCNP applied to PBMR, Master thesis, North-West University, 2009
- [11] Mohamad Hairie Rabir, Julia Abdul Karim and Mohd Amin Sharifuldin Salleh, Power and neutron flux calculation for the PuspatriTriga reactor using MCNP, *Jurnal Sains Nuklear Malaysia* 24 (2012) 22–32.
- [12] Istvan Rovni, Mate Szieberth, Laszlo Palcsu, Zoltan Major, Sandor Feher, High accuracy tritium measurement for the verification of the tritium production rate calculations with MCNPX, *Nuclear Instruments and Methods in Physics Research A* 714 (2013) 141–146.